CYBERNETICS AND PHYSICS, VOL. 13, NO. 4, 2024, 296–301

IDENTIFICATION OF NEURAL MASS NETWORK PARAMETERS USING EEG EVOKED POTENTIAL DATA

Sergei A. Plotnikov
Institute for Problems
of Mechanical Engineering
Saint-Petersburg, Russia
waterwalf@gmail.com

Article history:
Received 13.12.2024, Accepted 24.12.2024

Abstract

This paper describes an adaptive observer designed to estimate the parameters of neural mass networks. Neural mass populations describe the dynamics of cortical networks and are specifically designed to generate spontaneous electroencephalogram and evoked potentials – the brain's response to an external stimulus. The goal of this work is to adjust the parameters of neural mass models using electroencephalogram recordings from experiments on registering evoked potentials. Both a single neural mass population and the simplest network – two connected neural mass populations – are considered.

Key words

Neural mass model, electroencephalogram, evoked potential, adaptive observer, parameter identification, simulation

1 Introduction

An important problem at the intersection of several fields of science, such as neurobiology, physics and control theory, is the study of the neuronal activity of the human brain. On the one hand, it is important to study the causes of brain diseases such as epilepsy and schizophrenia [Milton and Jung, 2003; Ritsner, 2011] . On the other hand, understanding how the dynamics of brain rhythms change is important for predicting them. When implementing the neurofeedback paradigm – a psychophysiological procedure in which subjects are provided with models of neuronal activity for the purpose of regulating them online – delays associated with signal processing occur [Smetanin et al., 2018; Plotnikov et al., 2019]. To compensate for them, data obtained by predicting the dynamics of neuronal activity can be used. Both of these problems can be solved by synthesizing mathematical models of neuronal activity.

Electroencephalogram (EEG) is one of the simplest and most widely used methods for recording brain dynamics. It has a high temporal resolution but a fairly low spatial resolution. The advantages of this method include its non-invasiveness, meaning it can be used for almost any subject. However, because of this, the recorded signal is quite noisy. This method can be used to record both spontaneous EEG and evoked potentials (EP), which are specific changes in the EEG caused by external stimulation of sensory areas [Kropotov, 2009]. EEG and EP arise mainly due to the flow of extracellular current associated with the summed postsynaptic potentials in synchronously activated vertically oriented neurons. With the help of spontaneous EEG, it is possible to determine such diseases as epilepsy [Sharmila, 2018], Parkinson's disease [Silva et al., 2020], etc. The method of evoked potentials is used to diagnose such diseases as schizophrenia [Schielke and Krekelberg, 2022], attention deficit hyperactivity disorder [Meachon et al., 2021] and depression [Normann et al., 2007].

There are various mathematical models for describing neuronal activity. On the one hand, these can be networks of single-neuron models, such as the Hodgkin-Huxley [Hodgkin and Huxley, 1952], Hindmarsh-Rose [Hindmarsh and Rose, 1984], or FitzHugh-Nagumo [FitzHugh, 1961; Nagumo et al., 1962] models. Recent work has shown that the oscillations of a synchronized group of neurons can be described by the same equations as a single neuron, with the addition of noise [Panteley and Loría, 2017; Plotnikov and Fradkov, 2019]. Such synchronized groups of neurons form oscillators that generate brain rhythms[Gerster et al., 2020; Sevasteeva et al., 2021; Sevasteeva et al., 2022]. On the other hand, mathematical models can be used to describe the activity of the cortex. The best-known such model is the neural mass model (NMM) of Jansen and Rit [Jansen and Rit, 1995]. Some parameters of such models can be

calculated using anatomical data, while others are chosen experimentally.

This paper will be focused on the study of NMMs. Adaptive observers are used to estimate unknown parameters of the models. Some results on the synthesis of observers for NMMs were obtained in recent works [Postoyan et al., 2012; Liu et al., 2019; Sun and Liu, 2021; Plotnikov and Fradkov, 2024]. To adjust the model based on real data, the observer should use only its output, namely the potential difference in different areas of the brain. The best observer, in the author's opinion, for this problem is the one proposed in the work [Postoyan et al., 2012]. Therefore, it will be used to adjust the parameters in this paper. Note that there were attempts to use the observer proposed by the author [Plotnikov and Fradkov, 2024] to solve this problem, but they were unsuccessful.

2 Preliminaries

In this section, experimental EEG data, an overview of the NMM, and the adaptive observer proposed in [Postoyan et al., 2012] will be provided.

2.1 EEG data

EEG data was provided by the group of J.D. Kropotov from the N.P. Bechtereva Institute of the Human Brain, RAS. The recording of EP is considered as EEG data. Here it is a modification of the visual cued Go/NoGo paradigm described in [Kropotov and Mueller, 2009]. The trials consisted of presentations of two stimuli with an exposition of 100 ms and an interstimulus interval of 1000 ms. There were also inter-trial intervals of 3000 ms. The average result of 100 trials was considered as an EP recording, which is 3000 ms in length. The first stimulus starts at 300 ms.

A 19-channel EEG was recorded in the frequency band of $0.53 - 50$ Hz and sampled at a frequency of 250 Hz. The electrodes were placed according to the International $10 - 20$ system. The equipment included the Mitsar-201 electroencephalographic system (KE 0537) and the ELECTROCAP electrode cap with 19 tin electrodes. The channel under consideration is O1, which corresponds to the visual cortex.

2.2 Neural mass model

NMM describes the dynamics of a cortical column modeled by a population of pyramidal cells receiving excitatory and inhibitory feedback from local interneurons. Such a model can be used to model spontaneous EEG and EP of humans. The model is described by a system of six differential equations, which can be divided into three blocks that describe excitatory and inhibitory postsynaptic membrane potentials (PSPs).

$$\begin{aligned}
\dot{x}_1 &= x_2,\\
\dot{x}_2 &= Aa\sigma\left(x_3 - x_5\right) - 2ax_2 - a^2x_1,\\
\dot{x}_3 &= x_4,\\
\dot{x}_4 &= Aa\left[u + C_2\sigma\left(C_1x_1\right)\right] - 2ax_4 - a^2x_3,\\
\dot{x}_5 &= x_6,\\
\dot{x}_6 &= BbC_4\sigma\left(C_3x_1\right) - 2bx_6 - b^2x_5,
\end{aligned} \tag{1}$$

where $x = (x_1, \ldots, x_6)^{\mathrm{T}} \in \mathbb{R}^6$ is a state vector, while $y = x_3 - x_5 \in \mathbb{R}$ is the output of the whole system. Parameters A and B are proportional to the amplitude of PSP and differ for excitatory and inhibitory cases. Their standard values are $A = 3.25$ mV and $B = 22$ mV [Rotterdam et al., 1982], but they can change depending on several neuropeptides [Dodt et al., 1991]. Parameters a and b are inversely proportional to the duration of PSP and have fixed values: $a = 100\ \mathrm{s}^{-1}$, $b = 50\ \mathrm{s}^{-1}$ [Jansen et al., 1993]. Parameters C_1, C_2, C_3, and C_4 describe coupling forces for interconnection of pyramidal cells and excitatory and inhibitory interneurons. They are connected with each other as follows:

$$C_1 = \frac{5C_2}{4} = 4C_3 = 4C_4 = C,$$

where the value C defines the type of neural activity (the standard value is $C = 135$ to describe alpha rhythm) [Jansen and Rit, 1995]. The function

$$\sigma(v) = \frac{2e_0}{1 + \mathrm{e}^{r(v_0 - v)}},$$

is a sigmoid, which serves to transform the average membrane potential of a population of neurons into the average density of action potential impulses. Here $e_0 = 2.5\ \mathrm{s}^{-1}$, $r = 0.56\ \mathrm{mV}^{-1}$ and $v_0 = 6$ mV. u is represented by a pulse density which can be any arbitrary function including white noise. This input represents "spontaneous background" activity.

To simulate the EP, it is also necessary to add a signal describing the visual stimulus to the system input function u. This can be done using the function:

$$u_0(t) = \frac{q(t - t_0)^n\, \mathrm{e}^{(t_0 - t)/w}}{w^n}, \tag{2}$$

where $n = 7$, $w = 0.005$, $q = 0.5$, and t_0 is the moment of the stimulus (in seconds).

Throughout this paper, the value of C is assumed to be fixed. The goal is to adjust the values of parameters A and B.

2.3 Two coupled neural mass models

Certain EP components can depend on the interaction between two or more cortical columns. The visual cortex is responsible for processing visual information. It is mainly concentrated in the occipital lobe of each hemisphere of the brain and is linked to the prefrontal cortex via two other cortical areas: the prestriate cortex and the inferotemporal cortex. Thus, there is a delay for the visual signal to reach the visual cortex. The delays are

modeled by linear transformation but with latency three times longer, therefore $a_d \approx a/3$.

Here, two coupled NMMs are presented, which is a simplest case of a network:

$$\begin{aligned}
\dot{x}_1 &= x_2,\\
\dot{x}_2 &= Aa\sigma\left(x_3 - x_5\right) - 2ax_2 - a^2x_1,\\
\dot{x}_3 &= x_4,\\
\dot{x}_4 &= Aa\left[u + C_2\sigma\left(C_1x_1\right) + K_2x_{15}\right]\\
&\quad - 2ax_4 - a^2x_3,\\
\dot{x}_5 &= x_6,\\
\dot{x}_6 &= BbC_4\sigma\left(C_3x_1\right) - 2bx_6 - b^2x_5,\\
\dot{x}_7 &= x_8,\\
\dot{x}_8 &= Aa\sigma\left(x_9 - x_{11}\right) - 2ax_8 - a^2x_7,\\
\dot{x}_9 &= x_{10},\\
\dot{x}_{10} &= Aa\left[u_2 + C_2\sigma\left(C_1x_7\right) + K_1x_{13}\right]\\
&\quad - 2ax_{10} - a^2x_9,\\
\dot{x}_{11} &= x_{12},\\
\dot{x}_{12} &= BbC_4\sigma\left(C_3x_7\right) - 2bx_{12} - b^2x_{11},\\
\dot{x}_{13} &= x_{14},\\
\dot{x}_{14} &= Aa_d\sigma\left(x_3 - x_5\right) - 2a_dx_{14} - a^2x_{13},\\
\dot{x}_{15} &= x_{16},\\
\dot{x}_{16} &= Aa_d\sigma\left(x_9 - x_{11}\right) - 2a_dx_{16} - a^2x_{15},
\end{aligned} \tag{3}$$

Here, parameters A and B are supposed to be equivalent for each model. Each model has two inputs: an external one u, u_2, which can also be different for each model, and the output of the other model. Two connectivity constants, K_1 and K_2, attenuate the output of a column before it is transmitted to the other.

2.4 Adaptive observer

Both models (1) and (3) have the following general structure:

$$\begin{aligned}
\dot{x}_0 &= A_0x_0 + \varphi_0(y)\theta,\\
\dot{x}_1 &= A_1x_1 + \varphi_1(x_0,u)\theta,\\
y &= C_1x_1,
\end{aligned} \tag{4}$$

where $x_0 \in \mathbb{R}^{n_0}$, $x_1 \in \mathbb{R}^{n_1}$ are components of the state vector, $\theta \in \mathbb{R}^p$ is a vector of unknown constant parameters, $y \in \mathbb{R}$ is an output, and $u \in \mathbb{R}$ is an input.

For ease of notation, rewrite (4) in the following form:

$$\begin{aligned}
\dot{x} &= Ax + \varphi(y,u,x)\theta,\\
y &= Cx,
\end{aligned} \tag{5}$$

where $x = (x_0, x_1)$, $A = \operatorname{diag}(A_0, A_1)$, $C = (0, C_1)$ and $\varphi = (\varphi_0, \varphi_1)$. Nonlinear functions $\varphi_0 : \mathbb{R} \to \mathbb{R}^{n_0} \times \mathbb{R}^p$ and $\varphi_1 : \mathbb{R}^{n_0} \times \mathbb{R} \to \mathbb{R}^{n_1} \times \mathbb{R}^p$ are globally Lipschitz and bounded. Matrices A_0 and A_1 are Hurwitz.

Consider the following observer proposed in [Postoyan et al., 2012]:

$$\begin{aligned}
\dot{\hat{x}} &= A\hat{x} + \varphi(y,u,\hat{x})\hat{\theta} + \Gamma(y - \hat{y}),\\
\hat{y} &= C\hat{x},\\
\dot{\hat{\theta}} &= \bar{\Gamma}(y - \hat{y}),\\
\dot{\Psi} &= A\Psi + \Delta\varphi(y,u,\hat{x}),\ \Psi(0) = 0,\\
\dot{P} &= dP - dP\Psi^{\mathrm{T}}C^{\mathrm{T}}C\Psi P,\ P(0) = P(0)^{\mathrm{T}} > 0,
\end{aligned} \tag{6}$$

where $\Gamma = \Delta^{-1}\Psi\bar{\Gamma}$, $\bar{\Gamma} = P\Psi^{\mathrm{T}}C^{\mathrm{T}}$ and $\Delta = \operatorname{diag}(I_{n_0}, \frac{1}{d}I_{n_1})$, $d > 0$ is a constant parameter.

Theorem 1. *Let consider the system* (5) *and observer* (6). *Suppose that the following conditions are satisfied:*

1. *The vector of unknown parameters θ is constant and lies in a compact set.*
2. *The input u is known.*
3. *The output y does not contain noise.*
4. *For any signal u, y, $\hat{x}$ belonging to $\mathcal{L}_\infty$, there exist $a_1,\ a_2 \in \mathbb{R}_+$, $T \in \mathbb{R}_+$ such that the solution*

$$\dot{\Psi} = A\Psi + \Delta\varphi(y,u,\hat{x}),\ \Psi(0) = 0,$$

for all $t \geq 0$ satisfies the inequality:

$$a_1I_2 \leq \int_t^{t+T} \Psi^{\mathrm{T}}(\tau)C^{\mathrm{T}}C\Psi(\tau)\,\mathrm{d}\,\tau \leq a_2I_2.$$

Then there exsists $d^* \geq 1$ such that for all $d \geq d^*$ estimates $(\hat{x}, \hat{\theta})$ asymptotically tend to (x, θ). In other words, for all $d \geq d^*$, there exists $\beta_d \in \mathcal{KL}$ such that for all input u and any initial conditions $P(0) = P(0)^{\mathrm{T}} > 0$, $\tilde{x}(0)$, $\tilde{\theta}(0)$ the following inequality is fulfilled:

$$\left|\left(\tilde{x}(t), \tilde{\theta}(t)\right)\right| \leq \beta_d\left(\left|\left(\tilde{x}(0), \tilde{\theta}(0)\right)\right|, t\right), \quad \forall t \geq 0,$$

where $\tilde{x} = x - \hat{x}$, $\tilde{\theta} = \theta - \hat{\theta}$.

3 Main result

We begin our experiments with a simulation of the generation of EP using a single NMM (1). The standard values of parameters $A = 3.25$ and $B = 22$ are chosen, and initial conditions $x(0)$ are normally distributed with mean 0 and variance 1. The input u is Gaussian noise with a mean of 100 and a variance of 30^2. Also, input u contains two visual stimuli (2) at the moments of time $t_0 = 300$ and $t_0 = 1400$ ms. The simulation duration is 3000 ms, which corresponds to the EEG recording. To observe the results of parameter adjustment after the transient period, we consider a longer output y, which is obtained by concatenating the equivalent outputs of duration 3000 ms.

The goal is to determine the unknown to observer parameters A and B using only the output y of the NMM. The initial conditions for the observer are as follows: $\hat{x}(0) = 0$, $\hat{\theta}(0) = 0$, $\Psi(0) = 0$ and

$$P(0) = \begin{bmatrix} 4 & 1 \\ 1 & 5 \end{bmatrix}.$$

The designer parameter d is equal to 2.

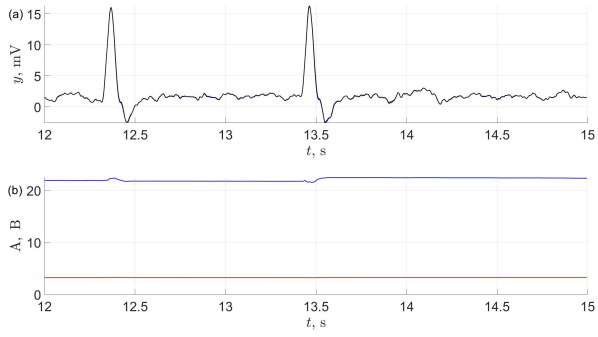

Figure 1. Adjustment of unknown parameters in the NMM (1) using its output: (a) Dynamics of the NMM output y (black), dynamics of the observer (6) output $\hat{y}$ (blue). (b) Dynamics of tunable parameters A (red) and B (blue).

Results of the simulation are shown in Fig. 1. The transient period is omitted. In Fig. 1(a), the black curve corresponds to the output y of the NMM (1), while the blue curve represents the output $\hat{y}$ of the observer (6). It can be seen that these two outputs almost coincide. There are two pronounced spikes corresponding to the visual stimuli (2). Figure 1(b) shows the dynamics of two adjustable parameters, A (red) and B (blue). Their average values are $A = 3.25$ and $B = 22.09$, respectively. It can be observed that the estimated parameters converge to the true values.

Now we use the EEG recording instead of the NMM output y. The EEG signal was filtered using a fourth-order Butterworth filter [Rabiner, 1975] to extract noise (in this case, a signal with a frequency greater than 30 Hz). To obtain the input u, the extracted noise was multiplied by 200 and 100 was added to it to produce noise similar to that in previous expirement. Note that due to latency, the reaction to the stimulus in the real data is delayed by approximately 70 ms. Therefore, the added visual stimuli (2) should be at time points $t_0 = 370$ and $t_0 = 1470$ ms.

Figure 2 shows the results of the simulation. The transient period is also omitted. In Fig. 2(a), the black curve corresponds to the experimental data (the average recording of EP from channel O1), and the blue curve represents the output $\hat{y}$ of the observer (6), as before. Tunable parameters A and B, presented in Fig. 2(b), do not tend to constant values, but we can calculate their average values: $A = 2.54$, $B = 22.8$. The red curve in Fig. 2(a) shows the dynamics of the output y of NMM with the obtained average parameters. It can be seen that this model simulates the upper spikes well, but does not cover the low-frequency dynamics. This is because we chose the value $C = 135$ for generating alpha activity (signal with a frequency of $8 - 12$ Hz), but EEG recording contains all rhythms (signal with a frequency of $0.53 - 50$ Hz).

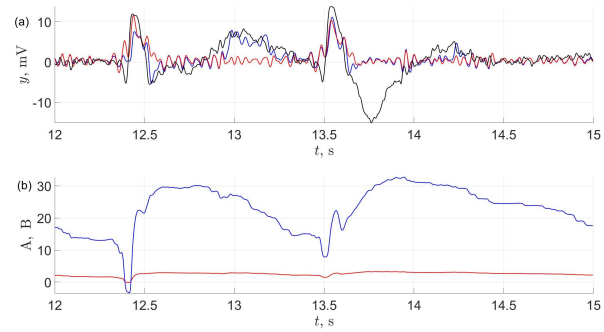

Figure 2. Adjustment of unknown parameters in the NMM (1) using real data: (a) EEG recording (black), dynamics of the observer (6) output $\hat{y}$ (blue), dynamics of the NMM output y (red) with obtained average parameters A and B. (b) Dynamics of tunable parameters A (red) and B (blue).

To account for the delay that occurs during visual signal transmission, we can consider two coupled NMMs (3). The values of parameters and initial conditions are the same as in the first experiment, with $K_1 = 1400$, $K_2 = 100$, and $a_d = 30$. The input to the second column, u_2, is the same as u, but it does not contain the visual stimuli (2). We will study how the reaction to the visual stimuli is transferred to the second model.

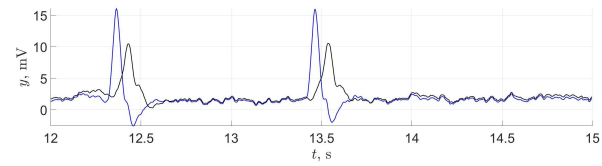

Figure 3. Dynamics of outputs from two coupled NMMs (3): output of the first NMM (blue), output of the second NMM (black).

This is shown in Fig. 3: one can see that the output of the second NMM (black) also reacts to the visual stimuli, although its input does not include them. There is a delay in the reaction of approximately 70 ms, which is comparable to the delay observed in experimental data.

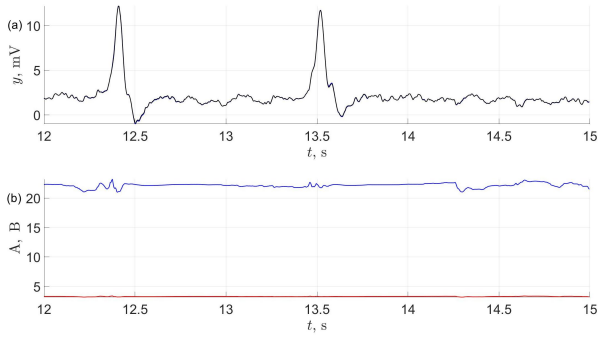

Figure 4. Adjustment of unknown parameters in two coupled NMMs (3) using the output of the second column: (a) Dynamics of the second NMM output y (black), dynamics of the observer (6) output $\hat{y}$ (blue). (b) Dynamics of tunable parameters A (red) and B (blue).

Now we can check how the observer (6) copes with this problem. The parameters A and B are assumed to be unknown. The initial conditions for the observer remain the same as before. The simulation results are shown in Fig. 4 (the transient period is always omitted). In Fig. 4(a), the black curve corresponds to the output y of the second NMM (3), while the blue curve represents the output $\hat{y}$ of the observer (6). As before, these two outputs almost coincide. Figure 4(b) shows the dynamics of two adjustable parameters, A (red) and B (blue), whose average values are $A = 3.25$ and $B = 22.14$, respectively: the estimated parameters converge to the true values.

The last experiment deals with a real data: the EEG recording is used instead of the second NMM output y. The input u and u_2 are the extracted noise multiplied by 200 and 100 added to it. The visual stimuli (2) added only to the input of the first NMM u at time points $t_0 = 300$ and $t_0 = 1400$ ms excluding delay.

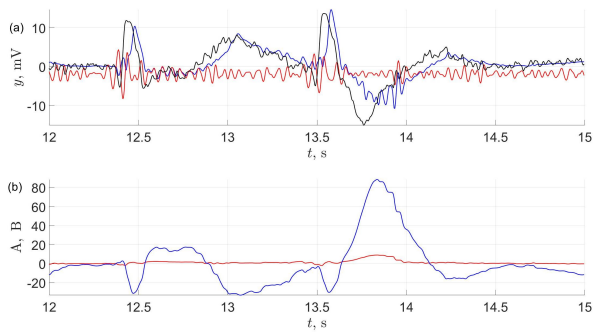

Figure 5. Adjustment of unknown parameters in two coupled NMMs (3) using real data: (a) EEG recording (black), dynamics of the observer (6) output $\hat{y}$ (blue), dynamics of the second NMM output y (red) with obtained average parameters A and B. (b) Dynamics of tunable parameters A (red) and B (blue).

Figure 5 shows the results of the simulation with the transient period omitted. In Fig. 5(a), the black curve corresponds to the experimental data, and the blue curve represents the output $\hat{y}$ of the observer (6), as before. Tunable parameters A and B, presented in Fig. 5(b), also do not tend to constant values and have the following average values: $A = 1.32$, $B = 0.98$. The red curve in Fig. 5(a) shows the dynamics of the output y of the second NMM with the obtained average parameters. In this experiment, one can see that model (3) captures the delay arising from the visual signal transmission. The output $\hat{y}$ of the observer (6) repeats the recording's dynamics quite well. However, simulating the output of two coupled NMMs with the obtained average parameters did not yield good results.

4 Conclusion

In this paper, it is shown that the observer proposed in [Postoyan et al., 2012] can be used to adjust the parameters of NMMs. This is true for both cases: when using the model's output and when working with EEG data in the case of recording EPs. The analysis includes situations with a single model and with two coupled NMMs. When the parameters are adjusted based on the output of the NMM, the observer accurately estimates them. This applies to both scenarios: one population and two coupled populations.

When considering the adjustment of parameters for a single NMM using EEG data, it is necessary to take into account the 70 ms delay that occurs during signal transmission. In this case, we can calculate the average parameter values at which the NMM will replicate the original EEG signal but without accounting for the low-frequency component. This is because, with fixed parameters, the NMM generates one rhythm, while the recording of real data is a signal containing all frequencies.

If we consider adjusting the parameters of two coupled NMMs using EEG data, modeling is performed without taking into account the delay. In this scenario, the observer replicates the dynamics of the original signal quite well, but with constant parameter values, the model produces a signal that does not resemble the original data.

Acknowledgment

This work was carried out at the Institute for Problems of Mechanical Engineering under the support of the Russian Science Foundation (Project No. 23-41-00060).

References

Dodt, H. U., Pawelzik, H., and Zieglgansberger, W. (1991). Actions of noradrenaline on neocortical neurons in vitro. *Brain Res.*, **545**, pp. 307–311.

FitzHugh, R. (1961). Impulses and physiological states in theoretical models of nerve membrane. *Biophys. J.*, **1** (6), pp. 445–466.

Gerster, M., Berner, R., Sawicki, J., Zakharova, A., Škoch, A., Hlinka, J., Lehnertz, K., and Schöll, E. (2020). FitzHugh–Nagumo oscillators on complex networks mimic epileptic-seizure-related synchronization phenomena. *Chaos*, **30** (12), pp. 123130.

Hindmarsh, J. L. and Rose, R. M. (1984). A model of neuronal bursting using three coupled first order differential equations. *Proc. R. Soc. Lond. B Biol. Sci.*, **221** (1222), pp. 87–102.

Hodgkin, A. L. and Huxley, A. F. (1952). A quantitative description of membrane current and its application to conduction and excitation in nerve. *J.Physiol.*, **117** (4), pp. 500–544.

Jansen, B. and Rit, V. (1995). Electroencephalogram and visual evoked potential generation in a mathematical model of coupled cortical columns. *Biol. Cybern.*, **73** (4), pp. 357–366.

Jansen, B., Zouridakis, G., and Brandt, M. E. (1993). A neurophysiologically-based mathematical model of flash visual evoked potentials. *Biol. Cybern.*, **68** (3), pp. 275–283.

Kropotov, J. D. (2009). *Quantitative EEG, event-related potentials and neurotherapy*. Elsevier, London.

Kropotov, J. D. and Mueller, A. (2009). What can event related potentials contribute to neuropsychology. *Acta Neuropsychol.*, **7**, pp. 169–181.

Liu, X., Sun, C.-X., Gao, Q., and Chen, Z.-W. (2019). A passivity-based observer for neural mass models. *IMA J. Math. Control. Inf.*, **36** (3), pp. 701–711.

Meachon, E. J., Meyer, M., Wilmut, K., Zemp, M., and Alpers, G. W. (2021). Evoked potentials differentiate developmental coordination disorder from attention-deficit/hyperactivity disorder in a stop-signal task: a pilot study. *Front. Hum. Neurosci.*, **15**.

Milton, J. and Jung, P., editors (2003). *Epilepsy as a dynamic disease*. Springer, Berlin.

Nagumo, J., Arimoto, S., and Yoshizawa, S. (1962). An active pulse transmission line simulating nerve axon. *Proc. IRE*, **50** (10), pp. 2061–2070.

Normann, C., Schmitz, D., Fürmaier, A., Döing, C., and Bach, M. (2007). Long-term plasticity of visually evoked potentials in humans is altered in major depression. *Biol. Psychiatry*, **62** (5), pp. 373–380.

Panteley, E. and Loría, A. (2017). Synchronization and dynamic consensus of heterogeneous networked systems. *IEEE Trans. Automat. Control*, **62** (8), pp. 3758–3773.

Plotnikov, S. A. and Fradkov, A. L. (2019). On synchronization in heterogeneous FitzHugh-Nagumo networks. *Chaos Soliton. Fract.*, **121**, pp. 85–91.

Plotnikov, S. A. and Fradkov, A. L. (2024). Adaptive parameter identification for a class of neural mass models with application to ergatic systems. *Mekhatronika, Avtomatizatsiya, Upravlenie*, **25** (1), pp. 13–18.

Plotnikov, S. A., Lipkovich, M., Semenov, D. M., and Fradkov, A. L. (2019). Artificial intelligence-based neurofeedback. *Cybernetics and Physics*, **8** (4), pp. 287–291.

Postoyan, R., Chong, M., Nesic, D., and Kuhlmann, L. (2012). Parameter and state estimation for a class of neural mass models. In *51th IEEE Conf. on Decis. Cont.*, pp. 2322–2327.

Rabiner, L. (1975). *Theory and application of digital signal processing*. Prentice-Hall, Englewood Cliffs, N.J.

Ritsner, M. S., editor (2011). *Handbook of schizophrenia spectrum disorders, volume I*. Springer, Dordrecht.

Rotterdam, A. v., Lopes da Silva, F. H., Ende, J. v. d., Viergever, M. A., and Hermans, A. J. (1982). A model of the spatial-temporal characteristics of the alpha rhythm. *Bull. Math. Biol.*, **44**, pp. 283–305.

Schielke, A. and Krekelberg, B. (2022). Steady state visual evoked potentials in schizophrenia: a review. *Front. Neurosci.*, **16**.

Sevasteeva, E. S., Plotnikov, S. A., and Belov, D. R. (2022). Gamma rhythm analysis and simulation using neuron models. *IFAC-PapersOnLine*, **55** (20), pp. 576–581.

Sevasteeva, E. S., Plotnikov, S. A., and Lynnyk, V. (2021). Processing and model design of the gamma oscillation activity based on FitzHugh-Nagumo model and its interaction with slow rhythms in the brain. *Cybernetics and Physics*, **10** (4), pp. 265–272.

Sharmila, A. (2018). Epilepsy detection from EEG signals: a review. *J. Med. Eng. Technol.*, **42** (5), pp. 368–380.

Silva, G., Alves, M., Cunha, R., Bispo, B. C., and M., R. P. (2020). Parkinson disease early detection using EEG channels cross-correlation. *Int. J. Appl. Eng. Res.*, **15** (3), pp. 197–203.

Smetanin, N., Lebedev, M., and Ossadtchi, A. (2018). Towards zero-latency neurofeedback. *bioRxiv*.

Sun, C.-X. and Liu, X. (2021). A state observer for the computational network model of neural populations. *Chaos*, **21**, pp. 013127.